

# A Novel Reconfiguration Method Using Image Processing Based Moving Shadow Detection, Optimization, and Analysis for PV Arrays \*

MEHMET KARAKOSE, MEHMET BAYGIN, KORAY SENER PARLAK,  
NURSENA BAYGIN AND ERHAN AKIN

*Department of Computer Engineering*

*Firat University*

*Elazig, 23119 Turkey*

*E-mail: {mkarakose; mbaygin; kparlak; nbaygin; eakin}@firat.edu.tr*

Reconfiguration system, which increases the energy efficiency in photovoltaic (PV) systems, is a critical stage in terms of energy efficiency. In this study, a moving shadow analysis and a novel optimization based on the reconfiguration method are proposed. The proposed approach builds up a new configuration by incorporating the radiation values into the PV system. To this end, the system is divided into two parts: adaptive and fixed, with the help of switching matrices. Image processing is employed in the study to acquire shadows and their information. The clonal selection method, which is an artificial immune algorithm, is preferred as the optimization process. The method is tested on a real PV system of a matrix size of 3×4. Both the series-parallel (SP) and total-cross-tied (TCT) connections are used in the tests. Shadows cast on the PV system are monitored incessantly by a camera and a reconfiguration is applied according to a predefined time threshold. The tests, performed in real time, show that the proposed system is accurate and efficient. The proposed reconfiguration method provides 10-20% of the average energy extraction for the S&P and TCT configuration layout.

**Keywords:** image processing, reconfiguration, partial shading, photovoltaic systems, optimization, switching matrix

## 1. INTRODUCTION

Photovoltaic (PV) systems are the leading systems currently available among renewable energy source applications. Despite the fact that they are remarkably efficient, reliable and work properly, some external factors severely impair their performance. The major impairing factors include deteriorations on the panel surface (*e.g.* stains, spots, residuals, scratches), clouds casting shadows on the panels and full or partial shadows cast by nearby objects. An ideal PV system is expected to overcome these problems by an adaptive system and boost the energy extraction with a minimum cost. Advanced PV systems follow several methods to diminish the aforementioned negative effects and seek to maximize the performance/cost ratio.

The partial or full shadows on the panels are the main source of the loss in available power in PV systems [1, 2]. Even though there has been a significant boost in the amount of energy mustered from the PV panels, the effort to prevent the factors hindering the performance falls short. Many methods can lessen the negative effects in PV arrays.

---

Received January 20, 2017; revised April 21 & June 9, 2017; accepted June 11, 2017.

Communicated by Chia-Feng Juang.

\* This study has been supported by The Scientific and Technological Research Council of Turkey (TUBITAK 1001 Programme) under Research Project No. 112E214.

These include the Maximum Power Point Tracker (MPPT), returned energy architecture, and reconfiguration techniques proposed in the literature [1-3]. The MPPT usually comes first among these methods. The MPPT is maintained by utilizing a DC-DC converter and controlling the algorithm and the current and voltage values obtained from the panels [2, 3]. The main goal of MPPT is to attain MPP by tracking the terminal voltage and current. To attain MPP, the DC-DC converter and a MPPT algorithm between the PV module and load are employed [3].

Various MPP techniques are proposed in the literature. The most prominent methods are Hill Climbing (HC) [3], Perturb and Observe (P&O) [4, 5] and incremental conductance [6]. A more efficient hybrid structure is formed in one of the proposed methods by using these techniques [7]. The major problem with the MPPT methods is partial shading. In this case, the global peak point (GP) in the power voltage (P-V) curve cannot be determined. Consequently, the PV system produces less energy.

Another approach to overcome the negative effect of full or partial shading on PV panels is reconfiguration [8, 9]. In short, reconfiguration is the rearrangement of the panels in PV arrays within a presented topology (*e.g.*, Series-Parallel, Total-Cross-Tied). This process is usually carried out by using a switching matrix [10, 11]. The effects of any type of shadow on the panels could be eliminated by changing the electrical connections without any need of a rearrangement of the panel positions. Thus, the shadows on the panels can be relocated to any position by only altering the connections. Therefore, the amount of energy produced increases. Furthermore, the problems coming from the shading of the panels are mitigated in this way. Hence, it facilitates the detection of the GP more accurately and precisely.

Nguyen *et al.* proposed an adaptive reconfiguration method in [12]. Two different configuration approaches are presented in this paper. In the first approach, before applying the switching of the adaptive array, a bubble sort algorithm is used to find the optimal panel layout. In the second approach, a reference model of power levels of each fixed panel row is used to estimate the power levels of the current panels. Karakose *et al.* utilizes an image processing algorithm in [13]. A camera constantly monitors the PV array and shadows casting on panels are detected with this approach. Then, radiation values of the panels are evaluated. The optimal panel layout is determined by basing on the radiation values and it is realized by altering the switching matrix accordingly. Liu *et al.* considers the shading degree for the reconfiguration. To accomplish this, Liu *et al.* determines the shadows formed on the rows in the first stage. The shading degrees in these rows are then determined by a sorting algorithm. In the second stage, the switching matrix connects an adaptive part to a fixed part of the PV arrays, based on the shading-degree control algorithm [14]. El-Dein *et al.* proposed a new mathematical formula for a reconfiguration [15]. Moreover, the branch and bound algorithm were used to determine the optimal layout. The fully or partially reconfigurable arrays are considered in the simulation studies for this paper. It is observed that the proposed approach provides an energy extraction between 10% and 20%. Cheng *et al.* has performed a fuzzy logic based reconfiguration process [16]. The shading degrees are used in this paper. The optimal panel layout is obtained by using fuzzy logic. It has been observed that the system provides fast and accurate responses in different environmental conditions. Karakose *et al.* presents a fuzzy partitioning based on the reconfiguration technique in another Karakose paper [17]. The short circuit current and radiation values of the panels are expressed

with fuzzy values. These are divided into five intervals. Storey *et al.* [18] proposed a dynamic cell configuration approach for an optimal energy output from the PV arrays. The system in this study has shown an average increase of 22.6% energy, as compared to the traditional approaches. Karakose *et al.* [19] utilizes the clonal selection algorithm for the reconfiguration. The calculation of the optimal panel layout is provided for energy extraction under the partial shading conditions in this paper.

The PV system experiences a significant loss of performance in conventional MPPT techniques, especially under full or partial shading conditions. This situation can be avoided through reconfiguration methods. The efficient operation of the reconfiguration and the MPPT techniques are very important and provide the following benefits:

- The energy obtained from the system increases.
- Cost/performance relationship develops.
- The negative effects of full or partial shading conditions are eliminated.

The amount of energy in the PV system is reduced significantly, as compared to the shading formed on the panels. The MPPT and reconfiguration techniques are used to overcome this situation. In this paper, a new approach, consisting of three steps, is proposed to reduce the negative effects of the full or partial shading conditions. In the first part of the proposed approach, the image processing algorithm is developed to detect the partial shading areas formed on the PV arrays. The boundaries, positions of the shadows and the radiation values of the panels are determined by using the image processing algorithm. Moreover, the period of the shadows is examined to help decide whether it is a permanent shadow or not. In the second part of the proposed technique, the new optimal layout is detected according to the radiation values obtained from the image processing algorithm by using the clonal selection algorithm. In the third part of the system, the control and decision algorithm was developed to determine the suitability of the optimal panel layout.

In this paper, the processing mechanism of the reconfiguration is described in Section 2. The image processing and optimization based reconfiguration algorithm is examined in Section 3. The experimental setup and results are presented in Section 4. The conclusions are discussed in Section 5.

## 2. RECONFIGURATION PROCESS

When full or partial shading occurs on PV arrays, the amount of current obtained from the shaded area is reduced significantly. This situation affects the amount of energy derived directly from the system in a negative way. The effect of shading occurring on the panels can be reduced by the reconfiguration. The results of the process show that some parameters are effective (*e.g.* systems connection type and environment temperature). Hence, an efficiency of about 5% to 40% can be achieved. There are several connection types for PV systems. However, when the studies in the literature were examined, two general connection types were observed: the series-parallel (S&P) and the Total-Cross-Tied (TCT) [12, 18].

*Series-Parallel (S&P)*: When all solar cells are a connected series, they are comprised of strings. These strings comprise the S&P type by connecting the parallel. The S&P connection type is presented in Fig. 1 (a).

*Total-Cross-Tied (TCT)*: When all solar cells are a connected parallel, they are comprised of modules. These modules comprise the TCT type by connecting the series. The TCT connection type is presented in Fig. 1 (b).

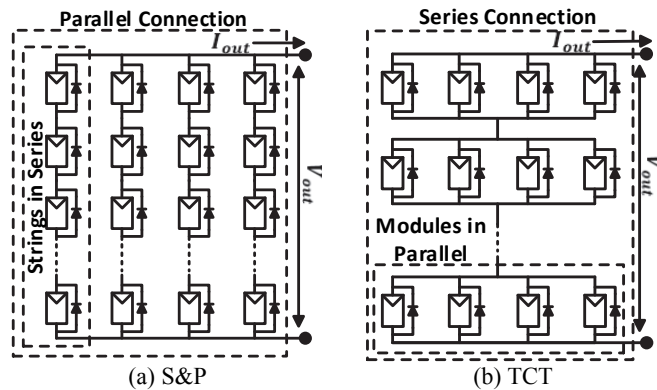
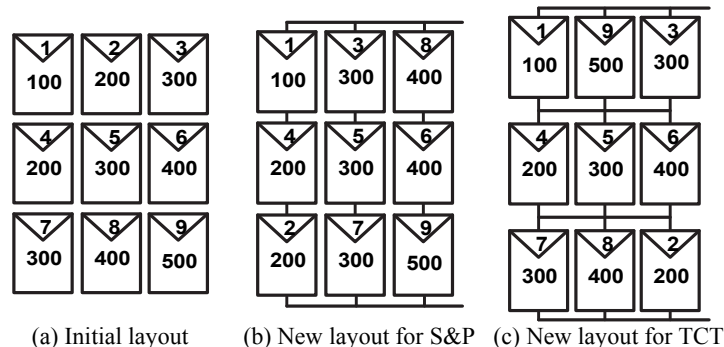


Fig. 1. The connection layout in PV systems.

The solar cells are connected in an S&P connection type. They are expected to have equal, or near equal, irradiation levels on each string. In the TCT connection type, the modules are expected to have an equal or close to equal radiation level with the reconfiguring. The block diagrams for the S&P [19] and TCT [20] connection types are presented in Figs. 2 (a)-(c).



(a) Initial layout (b) New layout for S&P (c) New layout for TCT  
Fig. 2. The connection configuration for energy extraction.

The most important module used for the reconfiguration is the switching matrix circuit. By using this module, entire electrical connections can be changed without any physical changes on the PV panels. The system is comprised of a fixed panel, an adap-

tive panel and a switching matrix circuit. The adaptive panel contains panels which have changeable connections. The fixed panel structure is always fixed and non-changeable [13, 21]. A schema of the switching matrix circuit used in a reconfiguration is presented in Fig. 3.

The radiation value formed on a PV module greatly affects the characteristics of the modules. In this case, the output current radiation-based equation [21] can be observed.

$$I_{ph} = \frac{G}{G_n} (I_{scn} + K_i (T - T_n)) \tag{1}$$

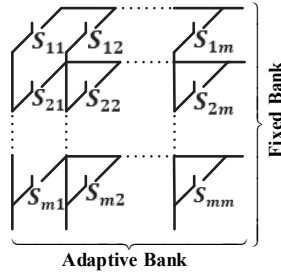


Fig. 3. The switching matrix circuit.

Here,  $I_{ph}$ , is a short circuit current of a PV cell;  $G_n$ , is a nominal radiance value,  $T_n$ , is the temperature value and  $K_i$  is the temperature coefficient of the short circuit current. In the literature, although there are different methods proposed for a reconfiguration, all of these methods have three main units: (1) adaptive and fixed panels; (2) a switching matrix circuit; and (3) a control unit [15, 21]. A common model for the TCT based reconfiguration is presented in Fig. 4.

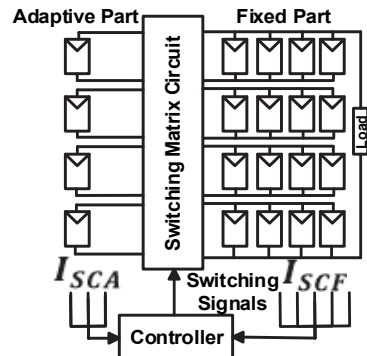


Fig. 4. The conventional reconfiguration method.

In this study, an alternative reconfiguration method is proposed. This method contains image processing and radiation values. The proposed approach has been observed to have good results for many shading conditions. The proposed method has several advantages; these include:

- There is no need for sensors to measure values, such as current and voltage.
- Implementation of the method is quite simple.
- It can work in a variety of environments and there is no need to edit it.

### 3. PROPOSED APPROACH

The proposed reconfiguration method has two fundamental steps: (1) Detection of the fully or partially shaded regions with an image processing algorithm and an evaluation of the shade degree; and (2) Decision of an optimum panel layout by using an artificial immune system. The panels are monitored continuously by a camera. Then the shadow is categorized as a temporary or a permanent shadow. If it is a permanent shadow, the radiation and the proportion of its area are evaluated and taken into consideration. Otherwise, it is ignored, because performing a reconfiguration for a brief shadow would cost more than the energy provided. The evaluated radiation and region information are fed into the second part of the method as two parameters. These parameters are used in the calculation of a new optimal arrangement. Moreover, in the second part of the proposed method, the control and decision-making module are located to test the applicability of the new PV layout. The general scheme of the proposed method is depicted in Fig. 5. The details of the algorithms will be elaborated upon in the following two sections.

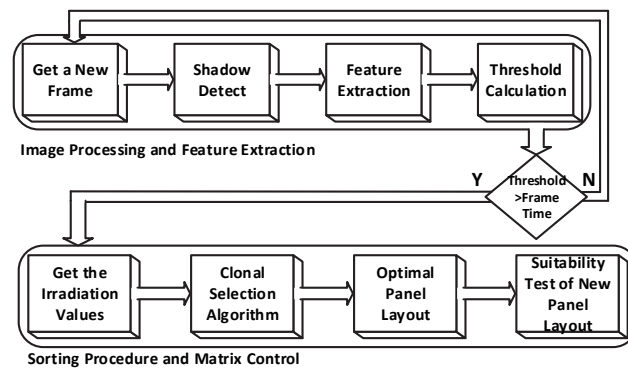


Fig. 5. The block diagram of proposed method.

#### (A) Image Processing Based Moving Shadow Analysis

The moving shadow analysis stage consists of two sections: (1) A camera continuously monitoring the PV arrays; and (2) An image processing module detecting a full or partial shading area. The image frames acquired from the camera are processed on an ARM based board. The shadows are categorized in this stage. The shadows are categorized according to time spent on the monitored region. If the shadow stays longer than an experimentally predefined threshold time, then it is considered a permanent shadow. As such, it is a necessary decision, because cloudiness varies during the daytime and clouds could cover the sun for a very short period of time. After this categorization, the features of the shadow are extracted. The contour of the shadow is determined by the Canny edge detection algorithm. The panels on which the shadow falls are then determined. The in-

tensity of the shadow and the size of its area are calculated. Lastly, the radiation values are evaluated from the information derived. In the conducted studies, the radiation values are completely obtained by the image processing algorithm. The shadows occurring on the panels are detected and the gray level of these shadows in the application is revealed. In addition, since the gray level values are proportional to the irradiation values, the irradiation value of the current panel can be obtained. In this process, the shadow densities occurring on the panels are calculated according to the gray levels and the radiation values are revealed. A block diagram outlining this process is presented in Fig. 6.

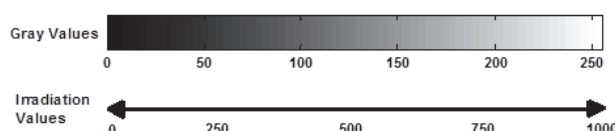


Fig. 6. Gray levels and radiation values.

Eq. (1) in Section 2 is used for the calibration and verification of the irradiation values obtained from the application. As it is mentioned in the beginning of the section, the detection of the shadows and analysis process are carried out by the image processing algorithm used in this paper. Firstly, an image frame is captured from the camera. Then, the image frame is converted into the HSV colour space. Several morphological methods, such as erosion and dilation, are subsequently applied. A noise reduction is performed on the image frames afterwards. Contour detection takes place next. It is carried out on the denoised frames. A Canny edge detection algorithm is used during the contour detection phase. It is reported that the Canny yields the best result among the other available edge detection algorithms (*e.g.* Sobel, Prewitt). The shadow is categorized by its level of darkness. The panels on which the shadow falls are determined in the next stage of the algorithm. Lastly, the total image frame time from the camera and the predetermined threshold time in the proposed approach are compared. This threshold value is a user-defined. Thus, it determines whether the shadows are temporary or permanent. The reason for the realization of this process is to avoid energy losses by continuously changing the state of the panels. This is because, during short time changes, an instantaneous change in the shadow values (sudden movement of the clouds, flying objects, *etc.*) will result in a certain loss of energy. As initially mentioned, this threshold used in the system is completely user-defined and is defined as 9 min for this study. In the measurements, the image taken and the elapsed time for processing it is approximately 600 ms. In this process, one image per second is taken. This process is carried out 540 times for 9 min. If the time calculated is higher than a threshold value, the shadow is considered a permanent shadow. The radiation and shadow area information derived are saved and later sent to the sorting and matrix control. Otherwise, the capturing of a new image frame will be conducted. A summary of the proposed algorithm is demonstrated in Fig. 7 (a). The stages of the image processing realizing this system is presented in Fig. 7 (b).

As seen in Fig. 7 (a), the system is constantly monitored and the shaded areas are detected. The radiation values obtained as a result of the image processing function are sent to the sorting procedure and matrix control function. Thus, optimization begins.

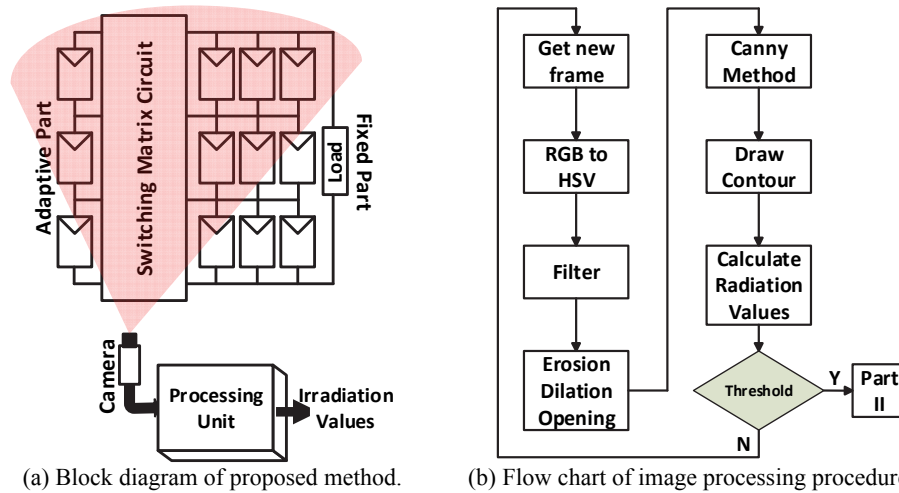


Fig. 7. Image processing part of the proposed method.

The image processing part is mainly comprised of 6 primary steps. These steps are as follows.

- **RGB to HSV conversion:** The first of these steps is converted into the HSV color space of the received image frame. The gray level color conversion is generally preferred in the literature. The HSV color space is an effective tool in revealing the shadows. HSV stands for Hue, Saturation and Value and is also often called HSB (B for brightness). In this paper, these three values are scaled between 0-255 and each value is determined individually.
- **Filter:** After the HSV conversion, a filter is applied to the image in the second step and an image frame is converted to a binary image. This conversion process is necessary for the erosion and dilation operations.
- **Erosion and Dilation:** The erosion and dilation operations are two basic morphological operations used to reveal the details in the image frame. If these two processes are performed in sequence, the noises in the image will be removed and the image will remain the same.
- **Opening:** After the erosion and dilation operations, the opening process is applied to the image frame in the fourth step. The opening process is useful to remove small objects. It is a combination of the erosion and dilation operations. The erosion operation is followed by the dilation operation. The opening procedure is presented in Eq. (2).

$$\text{Opening} = \text{Dilation}(\text{Erosion}(\text{frame})) \quad (2)$$

- **Canny Edge Detection and Draw Contour:** The shadows can be identified by using all of these steps. The boundaries of the shadow are detected by using the Canny algorithm. The determined boundaries are marked on the original image. The images summarizing all of these cases are provided in Figs. 8 (a)-(f).

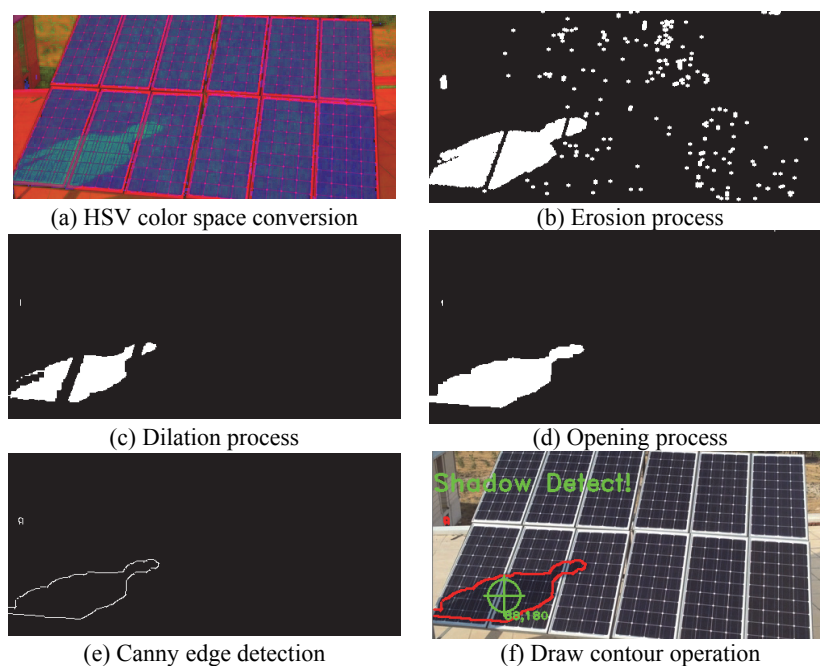


Fig. 8. Image processing steps in the proposed approach.

#### (B) Optimization Based Reconfiguration

The second part of the paper is the implementation optimization based reconfiguration. The radiation values obtained from the image processing are fed into the optimization algorithm. Therefore, the optimum panel arrangement is determined. The clonal selection algorithm is used as the optimization method. The algorithm takes the radiation values and the shaded region information as input parameters from the image processing part. The system that calculates the optimum arrangement of the panels by using these values proceeds with the sorting procedure and the matrix control. The purpose of this step is to choose the best combination of possible new panel layouts that will occur when the switching matrix is used. However, at this point, there is another problem arising: as the result of the optimization module is obtained, the new order cannot be provided, depending on the position of the switching matrix.

The optimization algorithms working principles do not always guarantee the best results. Therefore, the new panel layout obtained using a clonal selection algorithm may not be possible to be implemented with the system. To avoid this, a decision and control module are added to the optimization module. The optimization module calculates the best yield among all the possible locations of the switching matrix module. Then, the control and decision module takes this new panel layout as input parameters and tests the applicability of these possible combinations. If the new order is confirmed, the “True” value is produced and a new configuration performs. Otherwise, this module producing a “false” value returns to the optimization module and the panel. In this case, the result is a second best efficiency value presented to this module as an input parameter. A summary of the sorting and matrix control part is presented in Fig. 9.

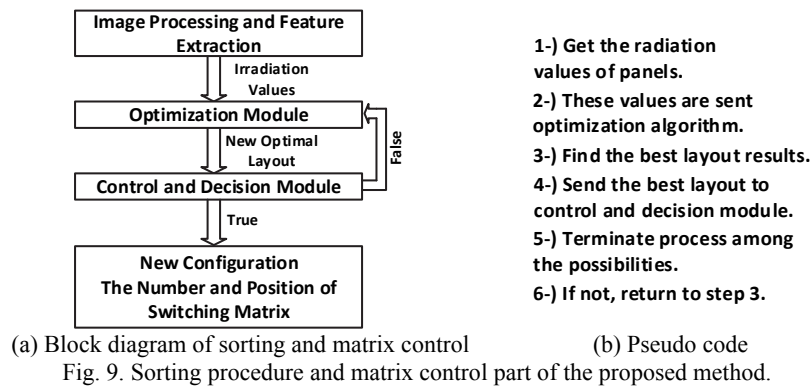


Fig. 9. Sorting procedure and matrix control part of the proposed method.

The implementation of the optimization module in the paper is compatible with both the S&P and TCT connection types. As is described in Section 2, for the S&P connection type, gathering the shadows in different regions into the same rows increases the energy extraction. The objective function of the S&P connection type is shown in Eq. (3). Conversely, for the TCT connection type, the even distribution of the shadows over the system is expected. In other words, every row is expected to have an equal or close to equal radiation level. The objective function suggested for the TCT connection type according to the radiation values is presented in Eq. (4).

$$SP_i = \min(RV_j), (i = 1, 2, \dots, m), (j = 1, 2, \dots, n) \quad (3)$$

$$Objective (SP) = \max\left(\sum_{i=1}^m SP_i\right)$$

Here, the  $SP_i$  is the minimum radiation value in the  $i$ th row on the PV system. The RV is the radiation values of the panels,  $m$  and  $n$  values is the count of row and columns.

$$TCT_i = \frac{\sum_{j=1}^n (RV_j)}{n}, (i = 1, 2, \dots, m) \quad (4)$$

$$Objective (TCT) = \min\left(\sum_{i=1}^{m-1} |TCT_{i+1} - TCT_i|\right)$$

In this paper, the clonal selection algorithm is used as the optimization method. The objective functions according to the type of connection for the S&P and TCT are utilized in Eqs. (3) and (4), respectively. The radiation values are considered to perform the optimization process. A block diagram illustrating the use in the working of the clonal selection algorithm is shown in Fig. 10.

In this paper, the clonal selection algorithm is preferred to detect the optimal panel layout. This algorithm consists of 5 basic steps. These steps are as follows:

- *Generate Initial Layout Randomly*: The first step of the algorithm is the formed population. The population size is set at 50. The permutation coding technique is used in the paper.

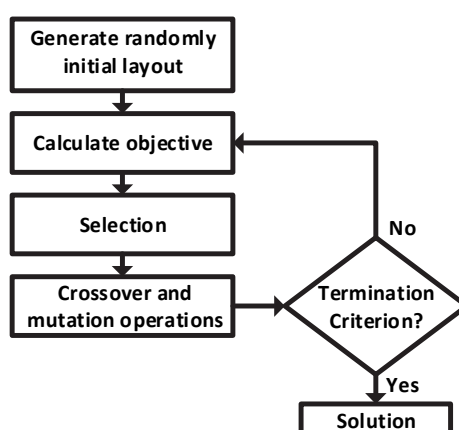


Fig. 10. Clonal selection algorithm for reconfiguration.

- *Calculate Objective*: In this part, Eqs. (3) and (4) are utilized as objective functions. These equations are called the fitness functions and are important for accuracy.
- *Selection*: The panel layouts with the best fitness values are selected in this step. The roulette wheel method is preferred, at this stage.
- *Crossover and Mutation Operations*: The selected panel layouts are used to create a new generation. The crossover and mutation operations are utilized to obtain new child individuals.
- *Termination Criterion*: This part is required to stop the algorithm. The number of iterations is used as the termination criteria and the iteration value is determined to be 550. If the algorithm reaches the endpoint, the optimal panel layout is presented as an input parameter to the switching matrix. Otherwise, the algorithm continues until it reaches the number of iterations.

The desired connection scheme can be obtained without the need to change any place in the PV systems by using the switching matrix. Theoretically, all connection variants may be obtained by applying a switching matrix between each module. This is not very practical in terms of both the complexity and the costs. Thus, one switching matrix is used in this paper and the position of this matrix in the system is constant. The schematic diagram of the switching matrix used in the system is presented in Fig. 11. Examples of the S&P and TCT connection types with a switching matrix are presented in Figs. 12 (a) and (b), respectively. Moreover, a list of possible connection configurations for both connection types are presented in Figs. 12 (c) and (d). As can be seen from Fig. 10, the switching matrix is arranged to divide the string for the S&P connection type. In this way, the changes between the strings can be performed. In the TCT connection type, the switching matrix is placed between the parallel modules and the adaptive bank is obtained. The possible combinations that can be obtained by using the switching matrix are the same in both connection types. In other words, the connection type does not affect the possible combinations that can be obtained in the PV systems.

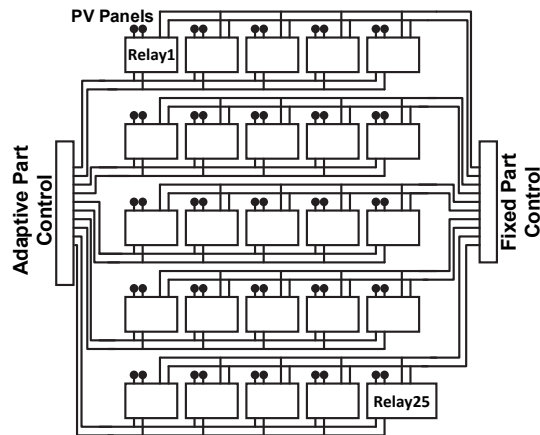
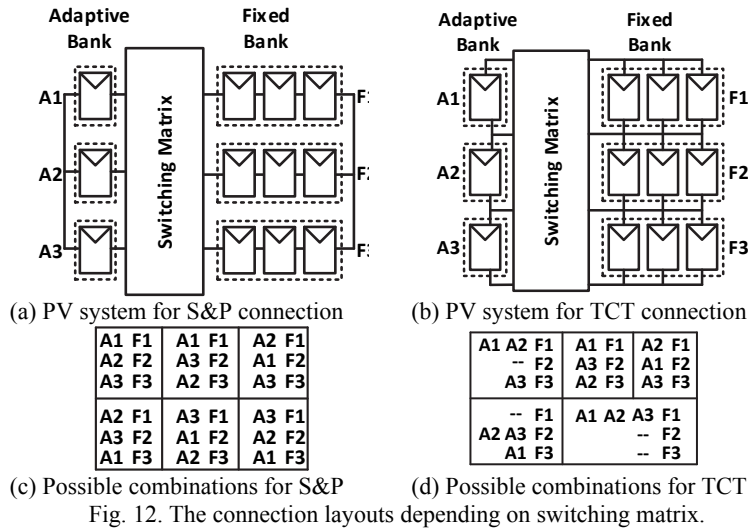


Fig. 11. The schematic diagram of the switching matrix.



(c) Possible combinations for S&P (d) Possible combinations for TCT

Fig. 12. The connection layouts depending on switching matrix.

### 4. EXPERIMENTAL RESULTS

Experiments were performed on a real PV system to verify the output of the proposed method. In this study, a PV system was established that was 3x4 in size. The connections were performed according to the S&P and TCT connection types. The system basically consists of 4 units: (1) the camera for the monitoring PV system; (2) the 3x4 PV panel system; and (3) an ARM based BeagleBoard XM card that performs image processing and control procedures; and (4) a switching matrix. The tests were conducted under the different shading conditions and temperatures. The applications were simulated in the MATLAB platform and the results were observed. A real experiment environment was then created for the reconfiguration in the PV systems. The validation of the

results obtained from the simulation were then performed. A block diagram illustrating the relationship between the test equipment is provided in Fig. 13.

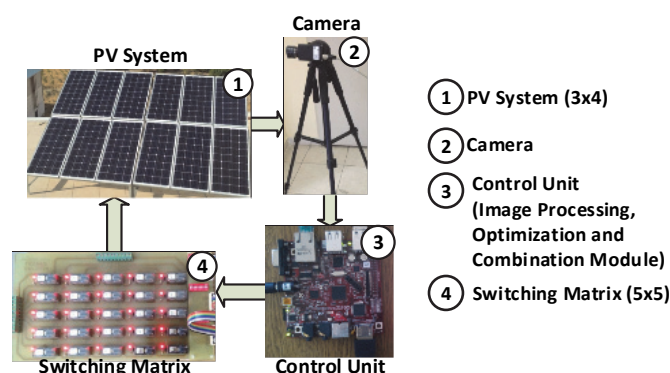


Fig. 13. The test equipment.

The system has the capacity to produce a total of approximately 1 kW. At this point, unlike in the studies in the literature, a large size is formed and the accuracy of the studies are carried out on this environment. The PV panels used in the system are Lorentz LC80-12M models. The characteristic features of these panels are presented in Table 1.

**Table 1. Characteristic features of PV panels.**

Electrical Data			Panel Features	
Feature	Unit	Value	Feature	Value
Peak power	Wp	80	Number of cells in series	36
Tolerance	%	+3/-3		
Max. power current	A	4.6	Number of cells in parallel	1
Max. power voltage	V	17.2		
Short circuit current	A	5.0	Cell technology	monocrystalline
Open circuit voltage	V	22.4		

As is seen in Fig. 13, the system consists of 4 main parts. The first part constitutes the PV system. There seems to be a 2×6 PV systems. The connections were carried out in the background according to the 3×4 layout. The panels also have bypass diodes. The numbered states and the connection order of these panels are presented in Fig. 14. In the imaging unit, the PV system is the section that continuously monitors. The camera is located and the imaging part transfers the controller board. The image is taken at regular intervals. In this control board, there is an image processing algorithm and an optimization algorithm to determine the optimal panel layout and the control and decision module to check the optimal panel layout. The fourth unit is the heart of the proposed approach. In this unit, the switching matrix takes information from the controller board as the input parameter to the control relays. In this way, the panels can be completely displaced electrically without the process of changing any physical location. The experimental results of the proposed approach will be presented in the two subsections: the image processing and the optimization algorithm.

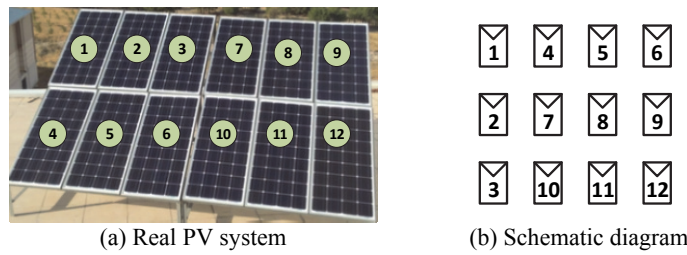


Fig. 14. Layouts of PV system.

(A) Shadow Analysis with Image Processing

The PV system with image processing applications is constantly monitored by using a camera. The radiation values of the panels are obtained. The Basler sca1600-28gc model cameras are used to monitor the system. The features of the camera and the experimental details of the image processing are presented in Table 2. Six examples is given for the S&P and TCT types between Figs. 15 and 20, and the outcomes obtained as a result of the image processing steps are shown in these figures.

**Table 2. Characteristic features of camera and experimental data.**

Camera Features		Experimental Features	
Feature	Value	Feature	Value
Resolution	1624×1234 px	Image Refresh Rate	1 image/sec
Frame Rate	28 fps		
Shutter Type	Global	Threshold Time (user-defined)	9 minute
Sensor Type	CCD		
Mono/Colour	Colour	Time of Day	01:00 p.m./04:00 p.m.
Interface	GigE		
Pixel Bit Depth	12 bits	Cloudiness of Day	Sunny, Partly Cloudy, Cloudy

Figs. 15-17 have been presented for the S&P connection type. The results reveal that shadows are detected. The gray level value is calculated with the image processing algorithm. The status of the shadow is analyzed with respect to time. T is a time where there is a user-defined threshold. According to this threshold time, it is decided as to whether the shading is temporary or not. Figs. 18-20 are presented for the TCT connection type. The radiation values of the sample cases are shown in Figs. 21 and 22 for the S&P and TCT connection types, respectively.

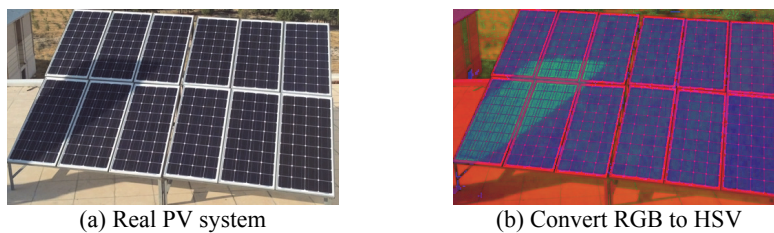
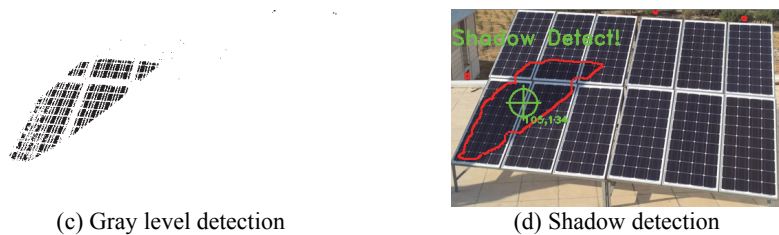
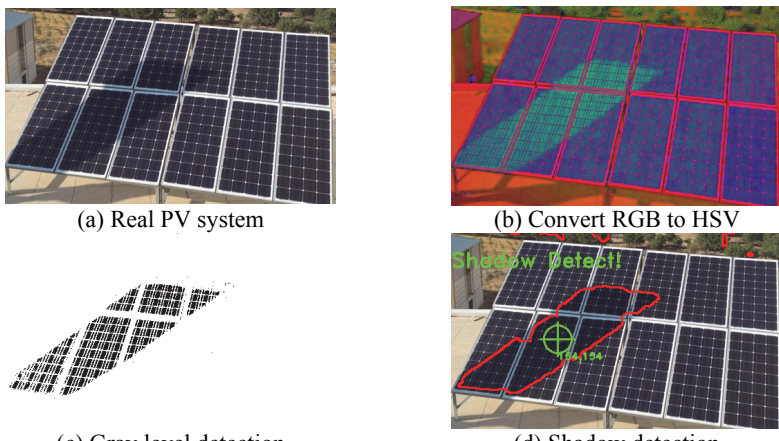


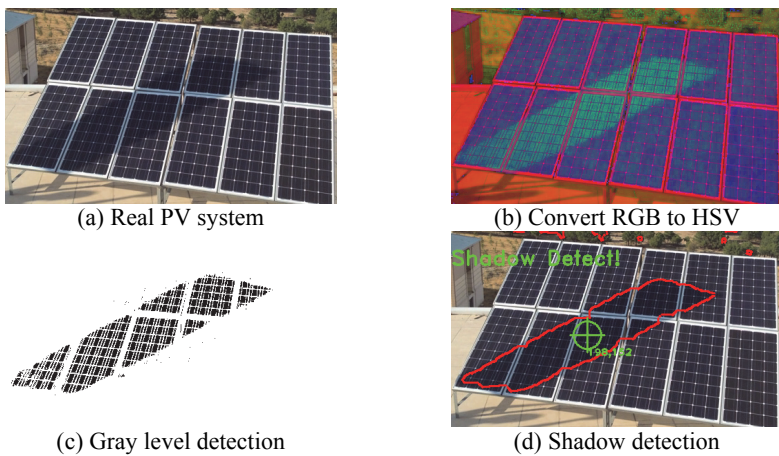
Fig. 15. The outputs obtained by image processing at time *t* for S&P type.



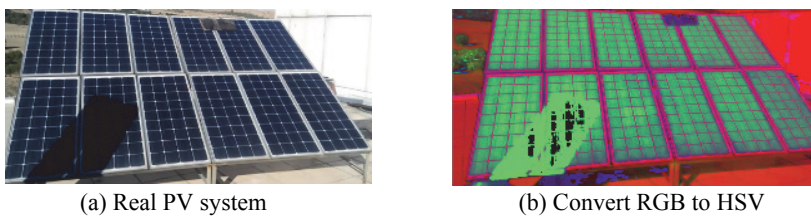
(c) Gray level detection  
Fig. 15. (Cont'd) The outputs obtained by image processing at time  $t$  for S&P type.



(a) Real PV system  
(b) Convert RGB to HSV  
(c) Gray level detection  
(d) Shadow detection  
Fig. 16. The outputs obtained by image processing at time  $t+1$  for S&P type.



(a) Real PV system  
(b) Convert RGB to HSV  
(c) Gray level detection  
(d) Shadow detection  
Fig. 17. The outputs obtained by image processing at time  $t+2$  for S&P type.



(a) Real PV system  
(b) Convert RGB to HSV  
Fig. 18. The outputs obtained by image processing at time  $t$  for TCT type.



Fig. 18. (Cont'd) The outputs obtained by image processing at time  $t$  for TCT type.

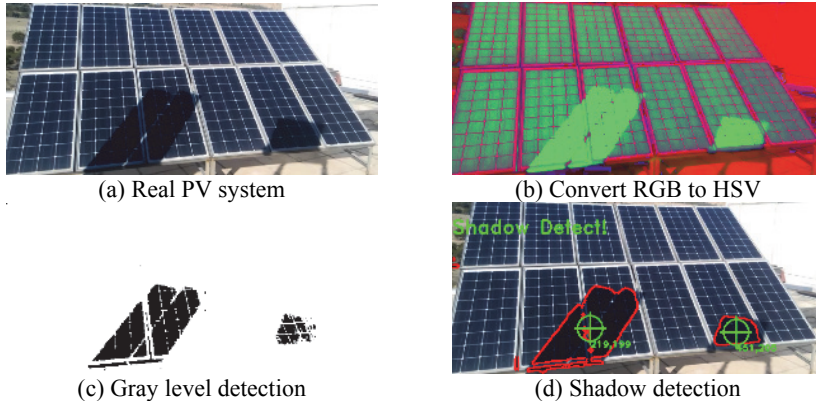


Fig. 19. The outputs obtained by image processing at time  $t+1$  for TCT type.

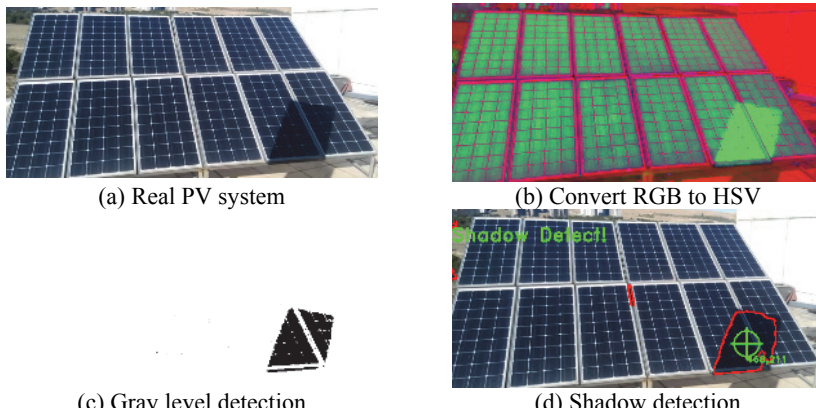


Fig. 20. The outputs obtained by image processing at time  $t+2$  for TCT type.

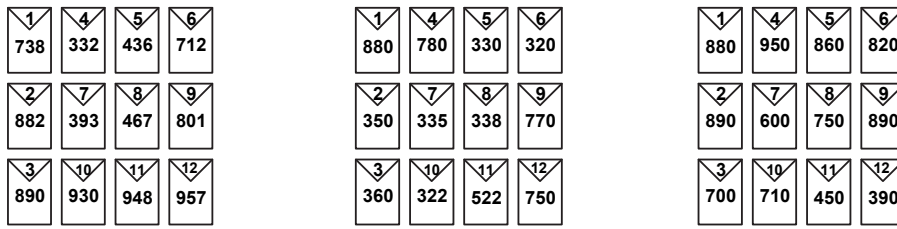
1 810	4 376	5 565	6 896
2 650	7 905	8 910	9 920
3 840	10 910	11 920	12 915

1 940	4 523	5 312	6 658
2 820	7 843	8 920	9 923
3 532	10 894	11 912	12 920

1 933	4 568	5 367	6 512
2 904	7 413	8 705	9 914
3 682	10 810	11 940	12 935

(a) Radiation values for Fig. 15. (b) Radiation values for Fig. 16. (c) Radiation values for Fig. 17.

Fig. 21. The radiation values for S&P connection types.

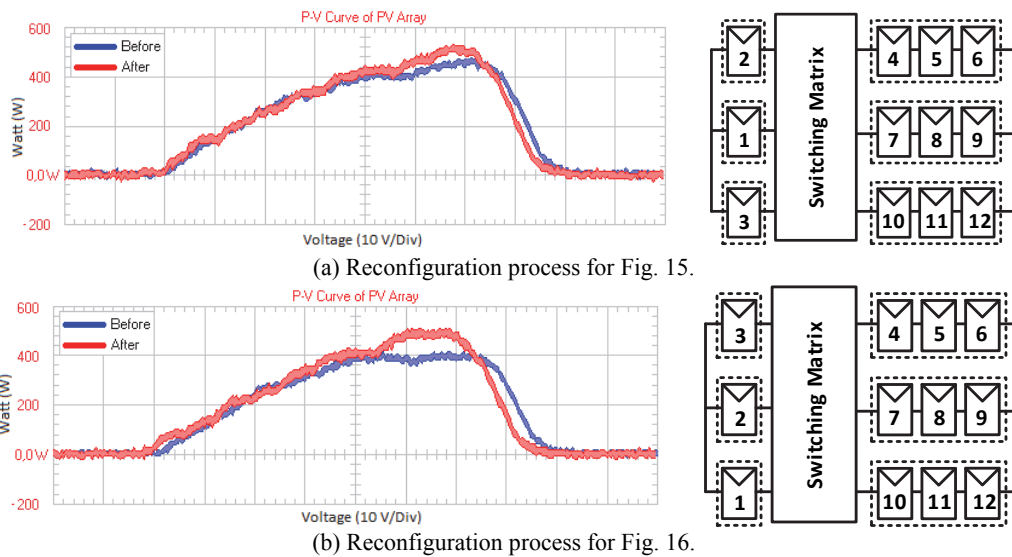


(a) Radiation values for Fig. 18. (b) Radiation values for Fig. 19. (c) Radiation values for Fig. 20.  
Fig. 22. The radiation values for TCT connection types.

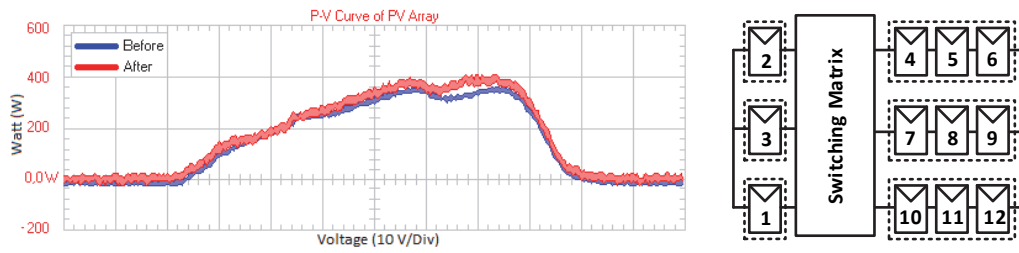
(B) Reconfiguration with the Clonal Selection Algorithm

In the reconfiguration part of this paper, the sorting and matrix control processes are performed by using radiation values obtained from the image processing. In this section, the optimization and control-decision module are used for the reconfiguration. The optimization module takes the radiation values of the panels as input parameters and yields an optimal panel layout as the output parameters. After this process, the control and decision module are activated. The control and decision module determine the optimal panel layout practically, whether it is provided or not, and if it is provided. The change of the power-voltage curves the things obtained from the PV system. The schematic block diagram of the new panel layout are presented in Fig. 23 for the S&P connection type. Also, the energy amount changes for this type of connection are presented in Table 3.

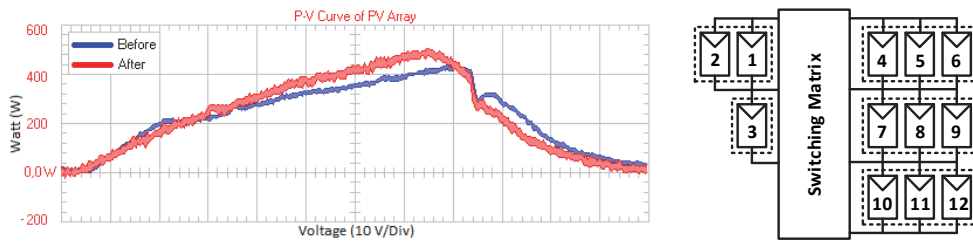
As seen in Fig. 23, the proposed method provides energy extraction at rates ranging from 10% to 25%. Figs. 23 (a)-(c) show the status in Fig. 21. They indicate the status of the energy and reconfiguration process at  $t$ ,  $t+1$  and  $t+2$ , respectively. The results obtained for the TCT connection layout are presented in Fig. 24. This figure illustrates the status of energy extraction for the TCT irradiation values presented in Fig. 22. The energy amount changes for TCT connection type are presented in Table 3.



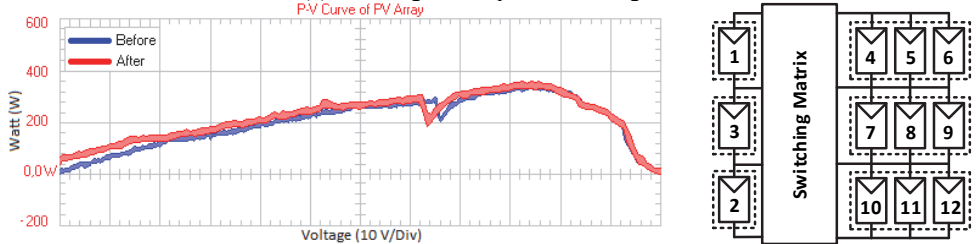
(a) Reconfiguration process for Fig. 15. (b) Reconfiguration process for Fig. 16.  
Fig. 23. Results of the reconfiguration for the S&P connection type.



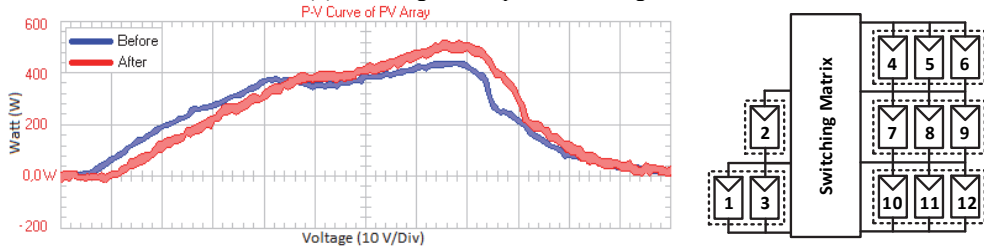
(c) Reconfiguration process for Fig. 17.  
 Fig. 23. (Cont'd) Results of the reconfiguration for the S&P connection type.



(a) Reconfiguration process for Fig. 18.



(b) Reconfiguration process for Fig. 19.



(c) Reconfiguration process for Fig. 20.

Fig. 24. Results of the reconfiguration for the TCT connection type.

**Table 3. Power variations for different connections.**

S&P				TCT			
Scenario	Before	After	Percent	Scenario	Before	After	Percent
Fig. 23 (a)	476 W	532 W	%11.8	Fig. 24 (a)	442 W	516 W	%16.7
Fig. 23 (b)	413 W	511 W	%23.7	Fig. 24 (b)	336 W	338 W	%0.6
Fig. 23 (c)	362 W	415 W	%14.6	Fig. 24 (c)	446 W	528 W	%18.4

The system is operated by a practical selection of the threshold time. The threshold time value is user-defined and may be determined in seconds or minutes. These values, determined as 9 minutes in this paper, and the status of the shading occurring within this time were examined. Consequently, the optimal layouts were applied to the system. Thus, there was an average increase of about 17% and 12% for the S&P and TCT connection layouts, respectively. The studies were carried out for both the S&P and TCT connection configurations. The proposed moving shadow analysis and optimization-based reconfiguration procedure were applied to 3×4 PV systems in real time; the effective results were obtained. The switching matrix is designed in a 5×5 size. But only part of the 3×4 designed switching matrix is used. The rest is an inactive state, and in the future, it will be used for larger PV systems. The results obtained from the proposed approach are expected to include larger changes with the larger system and the designing of the switching matrix, according to the scale of the system. The experimental results obtained from the proposed approach are presented comparatively in Table 4. The proposed method mainly consists of 3 modules. These are image processing, optimization and combination, and the switching matrix module, respectively. The operations performed on these modules are carried out on the control unit. The average time consumption of all these modules is given in Table 5. These time values may be better depending on the processor type. Also, performance values of the proposed approach for the larger PV arrays will be much better than the algorithms in the literature.

**Table 4. Performance comparison between our method and methods in the literature.**

Paper	Used Devices	Method	Connection	Performance (%)
[11]	Camera Current Sensor	Image Processing Fuzzy Logic	TCT	10
[13]	Camera	Image Processing	TCT	15
[17]	Current Sensor	Fuzzy Logic	S&P	11
[19]	Camera	Image Processing Fuzzy Logic	TCT	10
<b>This Paper</b>	Camera	Image Processing Optimization	<b>S&amp;P TCT</b>	<b>16.7</b>

**Table 5. Computational complexity of the proposed approach.**

Modules	Time Consumption (~ms)
Image Processing	~132 ms
Optimization and Combination	~89 ms
Switching Matrix	~32 ms
<b>Total</b>	<b>~253 ms</b>

## 5. CONCLUSIONS

In this study, a new method has been proposed to determine the full or partial shading situation and decrease the negative effects of these shadings. The shading occurring at any time during the day on PV arrays is detected by using image processing based on a shading analysis and obtained values for the shading area. The next step is to determine whether the shading is temporary or permanent. If it is temporary, the process

of a new frame is carried out, otherwise the optimization module is put into operation. The optimization module designed in this study can be used with both S&P and TCT connection types. The optimization module takes the radiation values as an input parameter. It then determines the best configuration. This configuration has been tested in combination with the availability of the module. After the process ends in the combination module, the new connection structure is applied on the switching matrix circuit and PV system, respectively. The proposed approach has 4 basic advantages: (1) it can be applied to both the S&P and TCT connection types; (2) the effects of shadings can be eliminated and there is no need for sensors for this process; (3) the system works according to the threshold value. Because of that, it doesn't commission unnecessary switching matrix circuits and it does not cause energy consumption; and (4) the efficiency of the method is validated with the experimental data, which yields a significant energy increase.

## REFERENCES

1. H. Patel and V. Agarwal, "MATLAB-based modeling to study the effects of partial shading on PV array characteristics," *IEEE Transactions on Energy Conversion*, Vol. 23, 2008, pp. 302-310.
2. A. Dolara, G. C. Lazaroiu, S. Leva, and G. Manzolini, "Experimental investigation of partial shading scenarios on PV (photovoltaic) modules," *Energy*, Vol. 55, 2013, pp. 466-475.
3. R. Rawat and S. S. Chandel, "Hill climbing techniques for tracking maximum power point in solar photovoltaic systems-a review," *International Journal of Sustainable Development and Green Economics*, Special Issue, Vol. 2, 2013, pp. 90-95.
4. N. Femia, G. Petrone, G. Spagnuolo, and M. Vitelli, "Optimization of perturb and observe maximum power point tracking method," *IEEE Transactions on Power Electronic*, Vol. 20, 2005, pp. 963-973.
5. N. Femia, G. Petrone, G. Spagnuolo, and M. Vitelli, "Predictive and adaptive MPPT perturb and observe method," *IEEE Transactions on Aerospace and Electronic Systems*, Vol. 43, 2007, pp. 934-950.
6. A. Safari and S. Mekhilef, "Simulation and hardware implementation of incremental conductance MPPT with direct control method using Cuk converter," *IEEE Transactions on Industrial Electronics*, Vol. 58, 2011, pp. 1154-1161.
7. L. L. Jiang, D. R. Nayanasiri, D. L. Maskell, and D. M. Vilathgamuwa, "A simple and efficient hybrid maximum power point tracking method for PV systems under partially shaded condition," in *Proceedings of the 39th International Annual Conference of the IEEE Industrial Electronics Society*, 2013, pp. 1513-1518.
8. P. Dos Santos, E. M. Vicente, and E. R. Ribeiro, "Reconfiguration methodology of shaded photovoltaic panels to maximize the produced energy," in *Proceedings of Brazilian Power Electronics Conference*, 2011, pp. 700-706.
9. G. Spagnuolo, G. Petrone, B. Lehman, C. A. R. Paja, Y. Zhao, and M. L. O. Gutierrez, "Control of photovoltaic arrays: Dynamical reconfiguration for fighting mismatched conditions and meeting load requests," *Industrial Electronics Magazine*, Vol. 9, 2015, pp. 62-76.
10. M. Balato, P. Manganiello, and M. Vitelli, "Fast dynamical reconfiguration algorithm of PV arrays," in *Proceedings of the 9th International Conference on Ecolog-*

- ical Vehicles and Renewable Energies*, 2014, pp. 1-8.
11. M. Karakose, M. Baygin, N. Baygin, K. Murat, and E. Akin, "Fuzzy based reconfiguration method using intelligent partial shadow detection in PV arrays," *International Journal of Computational Intelligence Systems*, Vol. 9, 2016, pp. 202-212.
  12. D. Nguyen and B. Lehman, "An adaptive solar photovoltaic array using model-based reconfiguration algorithm," *IEEE Transactions on Industrial Electronics*, Vol. 55, 2008, pp. 2644-2654.
  13. M. Karakose and M. Baygin, "Image processing based analysis of moving shadow effects for reconfiguration in PV arrays," in *Proceedings of IEEE International Energy Conference*, 2014, pp. 724-728.
  14. Y. Liu, Z. Pang, and Z. Cheng, "Research on an adaptive solar photovoltaic array using shading degree model-based reconfiguration algorithm," in *Proceedings of Control and Decision Conference*, 2010, pp. 2356-2360.
  15. M. Z. S. El-Dein, M. Kazerani, and M. M. A. Salama, "Optimal photovoltaic array reconfiguration to reduce partial shading losses," *IEEE Transactions on Sustainable Energy*, Vol. 4, 2013, pp. 145-153.
  16. Z. Cheng, Z. Pang, Y. Liu, and P. Xue, "An adaptive solar photovoltaic array reconfiguration method based on fuzzy control," in *Proceedings of the 8th World Congress on Intelligent Control and Automation*, 2010, pp. 176-181.
  17. M. Karakose, M. Baygin, N. Baygin, K. Murat, and E. Akin, "An intelligent reconfiguration approach based on fuzzy partitioning in PV arrays," in *Proceedings of IEEE International Symposium on Innovation in Intelligent Systems and Applications*, 2014, pp. 176-181.
  18. J. P. Storey, P. R. Wilson, and D. Bagnall, "Improved optimization strategy for irradiance equalization in dynamic photovoltaic arrays," *IEEE Transactions on Power Electronics*, Vol. 28, 2013, pp. 2946-2956.
  19. M. Karakose and K. Firildak, "A shadow detection approach based on fuzzy logic using images obtained from PV array," in *Proceedings of the 6th International Conference on Modeling, Simulation, and Applied Optimization*, 2015, pp. 1-5.
  20. G. V. Quesada, F. G. Gispert, R. P. Lopez, M. R. Lumbreas, and A. C. Roca, "Electrical PV array reconfiguration strategy for energy extraction improvement in grid-connected PV systems," *IEEE Transactions on Industrial Electronics*, Vol. 56, 2009, pp. 4319-4332.
  21. K. S. Parlak, "PV array reconfiguration method under partial shading conditions," *International Journal of Electrical Power and Energy Systems*, Vol. 63, 2014, pp. 713-721.



**Mehmet Karakose** received the B.S. degree in Electrical Engineering from Firat University, Elazig, Turkey, in 1998, the M.S. degree in Computer Engineering from Firat University, Elazig, Turkey, in 2001, respectively, and the Ph.D. degree in Electrical Engineering (Computer Engineering) from Firat University, Elazig, Turkey, in 2005. He is currently an Associate Professor Doctor in the Department of Computer Engineering, Firat University, Turkey. He was a research assistant at Computer Engineering Department, Firat University from 1999 to 2005. His research interests include fuzzy systems, intelligent systems, simulation and modeling, fault

diagnosis, computer vision, railway inspection systems, and photovoltaic systems. Dr. Karakose is an IEEE senior member.



**Mehmet Baygin** born in Elazig, Turkey, in 1988. He received the B.S. degree in Computer Engineering from Firat University, Elazig, Turkey, in 2010, the M.S. degree in Computer Engineering from Firat University, Elazig, Turkey, in 2013, respectively and he started the Ph.D. program in Computer Engineering from Firat University, Elazig, Turkey, in 2013. He is currently a Research Assistant in the Department of Computer Engineering, Ardahan University, Turkey. His research interests are image processing, computer vision, photovoltaic systems and heuristic methods.



**Koray Sener Parlak** was born in Elazig in 1974. He received BSc., M.Sc. and Ph.D. degrees in Electrical Engineering from Firat University (Elazig-Turkey) in 1996, 2000, 2006 respectively. He is currently working as an Associate Professor in Department of Electronic Automation in Technical Vocational High School at Firat University. His research interests are power systems, microgrids and PV systems.



**Nursena Baygin** born in Batman, Turkey, in 1987. She received the B.S. degree in Computer Engineering from Firat University, Elazig, Turkey, in 2011, and she started the M.S. program in Computer Engineering from Firat University, Elazig, Turkey, in 2013. She is currently a Research Assistant in the Department of Computer Engineering, Kafkas University, Turkey. Her research interests are optimization, image processing, photovoltaic systems and heuristic methods.



**Erhan Akin** was born in Erzincan, Turkey, in 1963. He received the B.S. and M.S. degrees in Electrical Engineering and the Ph.D. degree in the area of ac drives from Firat University, Elazig, Turkey, in 1984, 1987, and 1994, respectively. He was with the Department of Electrical Engineering, Firat University, first as an Assistant Professor and then as an Associate Professor of Electrical Machines. He is currently a Full Professor of Computer Engineering at Firat University. His main research interests are in power electronics, digital control of variable-speed ac drives, fuzzy control and soft-computing techniques.